

# Detonation Tube Impulse in Sub-atmospheric Environments

M. Cooper\* and J. E. Shepherd†

The thrust from a multi-cycle, pulse detonation engine operating at practical flight altitudes will vary with the surrounding environment pressure. We have carried out the first experimental study using a detonation tube hung in a ballistic pendulum arrangement within a large pressure vessel in order to determine the effect that the environment has on the single-cycle impulse. The air pressure inside the vessel surrounding the detonation tube varied between 100 and 1.4 kPa while the initial pressure of the stoichiometric ethylene-oxygen mixture inside the tube varied between 100 and 30 kPa. The original impulse model (Wintenberger et al., *Journal of Propulsion and Power*, Vol. 19, No. 1, 2002) was modified to predict the observed increase in impulse and blow down time as the environment pressure decreased below one atmosphere. Comparisons between the impulse from detonation tubes and ideal, steady flow rockets indicate incomplete expansion of the detonation tube exhaust, resulting in a 37% difference in impulse at a pressure ratio (ratio of pressure behind the Taylor wave to the environment pressure) of 100.

## Nomenclature

Roman Characters

$A$	area of steady flow nozzle exit
$c$	speed of sound
$F$	force
$F_D$	force due to diaphragm

---

\*Postdoctoral Appointee, Sandia National Laboratories, Albuquerque, NM, AIAA member

†Professor, California Institute of Technology, Pasadena, CA, AIAA member

$g$	gravitational acceleration
$h$	enthalpy per unit mass
$I$	impulse
$I_{SP}$	mixture-based specific impulse
$I_V$	impulse normalized by the tube volume
$K$	model proportionality constant
$K_{LP}$	variable model proportionality constant $K$ for low environment pressures
$L$	tube length
$L_p$	pendulum arm length
$\dot{m}$	mass flow rate
$M_p$	pendulum mass
$P$	pressure
$q$	effective energy release per unit mass of mixture
$R$	perfect gas constant
$T$	temperature
$t$	time
$t_1$	time taken by the detonation wave to reach the open tube end
$t_2$	time taken by the first reflected characteristic to reach the thrust surface
$t_3$	time associated with pressure decay period
$u$	velocity
$U_{CJ}$	CJ detonation velocity
$V$	tube volume

#### Greek Characters

$\alpha$	non-dimensional parameter corresponding to time $t_2$
$\beta$	constant non-dimensional parameter corresponding to pressure decay period
$\beta_{LP}$	variable non-dimensional parameter corresponding to pressure decay in low environment pressures
$\Delta x$	maximum horizontal displacement
$\gamma$	specific heat ratio

$\Pi$	non-dimensional pressure, $[P(t) - P_0]/[P_3 - P_0]$
$\rho$	density

#### Subscripts

0	state of environment
1	reactant state
2	CJ detonation state
3	state in stagnant flow region behind the Taylor wave
$t$	stagnation properties

## I. Introduction

The motivation for this study comes from the continued development of a novel propulsive device called a pulse detonation engine (PDE) which is based on intermittent detonation to generate quasi-steady thrust. Multi-cycle performance estimates<sup>1,2</sup> for fully-filled, air-breathing PDEs without exit nozzles currently exist for varying flight Mach numbers. These results suggest inefficient operation due to incomplete expansion of the exit flow yet no experimental data exist with which to validate these estimates.

In order for PDE performance to be comparable to existing propulsion systems, it has been proposed to use some type of exit nozzle. Known from the analysis of steady flow nozzles, the nozzle pressure ratio determines the nozzle effectiveness and depends directly on the environment pressure which varies as a function of altitude. Operation at higher altitude increases the nozzle pressure ratio enabling more thermal energy of the exhaust products to be converted into kinetic energy, thus increasing the thrust transferred to the engine. Before the effect of nozzles on detonation tubes can be quantified, the effect that the environment pressure has on the impulse from fully-filled, straight detonation tubes must be understood. The environment temperature also varies with altitude but this effect on impulse is beyond the scope of this work. The data presented here provide a baseline from which detonation tube nozzles can be evaluated and enable the effect of increased blow down time due to exhausting into lower pressures to be separated from the additional flow expansion provided by a nozzle. Comparisons of the detonation tube impulses to estimates assuming ideal steady flow provide a measure of detonation exhaust under-expansion. Although such a comparison is not strictly valid since the flow exhausting from a detonation tube is unsteady and not pressure matched to the environment, the observed differences suggest the magnitude of impulse that could possibly be gained by adding a perfectly designed nozzle.

Historically, single-cycle ballistic pendulum experiments have been instrumental in quan-

tifying the maximum impulses obtained for specific operating conditions which, until now, have only investigated in-tube parameters such as the initial pressure, equivalence ratio and diluent of the explosive mixture, internal obstacle configurations, and ignition sources. For this reason, we utilize the ballistic pendulum arrangement in conducting the first systematic experimental investigation of detonation tube impulse as a function of environment pressure. A simplified detonation tube, consisting of a cylinder closed at one end and open at the other, is used. The existing impulse model<sup>3</sup> is extended to also include the effect of environment pressure.

## II. Impulse Model for $P_0 \neq P_1$

A detonation tube is best analyzed with a control volume<sup>3</sup> that surrounds the tube walls (Fig. 1). The idealized thrust surface pressure history for the situation when  $P_0 \neq P_1$  is

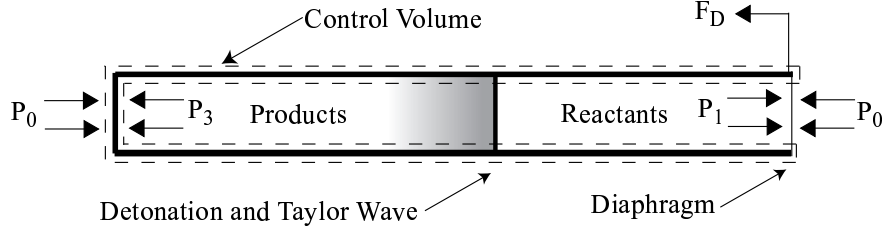


**Figure 1.** Illustration of detonation tube control volume when the initial combustible mixture is sealed inside the tube with a diaphragm and the detonation wave has not reached the open end.

illustrated in Fig. 2. The impulse is predicted by integrating the forces acting on the control volume of Fig. 1

$$I = \int_0^{\infty} \sum F dt = I_1 + I_2 + I_3 \quad (1)$$

and consists of contributions from the three time periods illustrated in Fig. 2.

During time period  $t_1 = L/U_{CJ}$ , the thrust surface experiences a force from the pressure differential  $P_3 - P_0$ , whereas the open tube end experiences a constant force from the pressure differential  $P_0 - P_1$ . This pressure difference at the open end is supported by the diaphragm which passes through the control surface (Fig. 1) generating a force  $F_D = \int_0^{t_1} (P_0 - P_1) \cdot A dt$ , not considered in previous impulse models<sup>4,3</sup>. The impulse integral during time  $t_1$  is

$$\begin{aligned} I_1 &= \int_0^{t_1} (P_3 - P_0) \cdot A dt + F_D = \int_0^{t_1} (P_3 - P_1) \cdot A dt = (P_3 - P_1) A t_1 \\ &= (P_3 - P_1)V/U_{CJ} \end{aligned} \quad (2)$$

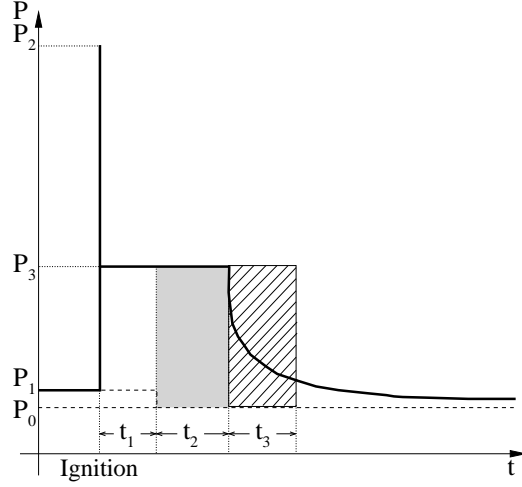


**Figure 2.** Idealized thrust surface pressure history for tubes with  $P_1$  not equal to  $P_0$ .

Time  $t_2$  is required for the reflected wave from the open tube end to reach the thrust surface. During this time, the thrust surface pressure history can be integrated directly from the pressure difference across the thrust surface and is scaled<sup>3</sup> with a non-dimensional parameter  $\alpha = t_2 c_3 / L$ .

$$\begin{aligned}
 I_2 &= \int_{t_1}^{t_1+t_2} (P_3 - P_0) \cdot A \, dt = (P_3 - P_0) A t_2 \\
 &= (P_3 - P_0) \alpha V / c_3
 \end{aligned} \tag{3}$$

During time  $t_3$ , the rate of pressure decay at the thrust surface is determined by the environment pressure and the relative sound speeds in the gases. The impulse  $I_3$  during this time is scaled<sup>3</sup> with the non-dimensional parameter  $\beta = \int_{\tau_1+\tau_2}^{\infty} \Pi(\tau) d\tau$ .

$$\begin{aligned}
 I_3 &= \int_{t_1+t_2}^{\infty} [P(t) - P_0] \cdot A \, dt = \frac{(P_3 - P_0) V}{c_3} \int_{\tau_1+\tau_2}^{\infty} \Pi(\tau) d\tau \\
 &= (P_3 - P_0) \beta V / c_3
 \end{aligned} \tag{4}$$

With the value of  $\beta$ , a characteristic time  $t_3 = \beta L / c_3$  is defined<sup>3</sup> that represents the hatched region in Fig. 2.

When  $P_0 = P_1$ , the pressure decay integral was assumed<sup>3</sup> to have a constant value of  $\beta = 0.53$ . Decreasing the environment pressure will increase the blow down time  $t_3$  along with the corresponding value of  $\beta$ . This increase in blow down time is evident from the measured thrust surface pressure histories, shown in Fig. 3, for environment pressures of 100 kPa and 1.4 kPa. Because the exhaust is choked throughout most of the process, the

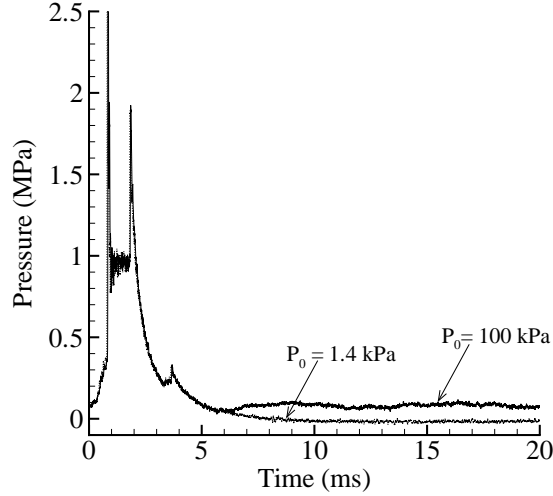


**Figure 3.** Measured thrust surface pressure histories with  $P_1 = 80$  kPa and  $P_0 = 100$  and 1.4 kPa.

pressures are identical until the value of  $P_0$  is nearly reached. The traces clearly show that additional time is required for the detonation tube to equilibrate to the lower environment pressures (approximately 5 ms for  $P_0 = 100$  kPa if not considering the under-pressure region and approximately 7.5 ms for  $P_0 = 1.4$  kPa). Thus, simply decreasing the environment pressure almost 100% causes a 50% increase in the blow down time. While this increase in blow down time positively affects the single-cycle impulse, it should be noted that the thrust of multi-cycle PDEs may be negatively affected if high cycle frequencies are required.

The three components of the impulse for times  $t_1$ ,  $t_2$ , and  $t_3$  are summed to yield the total specific impulse.

$$I_{SP} = \frac{I}{V\rho_1g} = \frac{K}{\rho_1gU_{CJ}}(P_3 - P_0) \quad (5)$$

This relationship for the impulse equals that previously determined by Wintenberger et al.<sup>3</sup> except now we find that  $K$  depends not only on the energy content  $q/RT_1$  and the specific heat ratio  $\gamma$  as was determined previously<sup>3</sup>, but also on the environment pressure  $P_0/P_1$ .

$$K = K(\gamma, q/RT_1, P_0/P_1) = \left[ \frac{(P_3/P_1 - 1)}{(P_3/P_1 - P_0/P_1)} + \alpha \frac{U_{CJ}}{c_3} + \beta \frac{U_{CJ}}{c_3} \right] \quad (6)$$

Equation 6 differs from the original impulse model<sup>3</sup> by the first term which was previously assumed to equal unity. The reader is referred to previous literature for a discussion of the effect of the specific heat ratio<sup>5,6</sup>  $\gamma$  and the specific energy content<sup>3</sup>  $q/RT_1$  while this study addresses the effect of  $P_0/P_1$  on the impulse and the parameter  $K$ . The values of  $K$  and  $\beta$  are determined from experimental data.

Decreasing the environment pressure in Eq. 5 increases the specific impulse (holding all else constant, including  $K$ ) which is due to an increase in the pressure difference  $P_3 - P_0$ . Changes in the environment pressure also affect the first and third terms of  $K$  (Eq. 6). The first term of  $K$  varies with the environment pressure only by variations in the  $P_0/P_1$  parameter. The pressure ratio  $P_3/P_1$  is known<sup>3</sup> to depend only on the properties (specific heat ratio  $\gamma$  and energy content  $q/RT_1$ ) of the initial mixture. Thus, decreasing  $P_0/P_1$  results in decreasing the first term of Eq. 6 for  $P_0/P_1 < 1$ . Decreasing  $P_0/P_1$  causes an increase in the third term of Eq. 6 by increasing  $\beta$ . It is this increase in  $\beta$  (representing the blow down time) that causes the measurable increases in  $K$  and  $I_{SP}$  to occur. Thus, the specific impulse of a detonation tube depends on the mixture properties ( $\gamma$  and  $q/RT_1$ ), and the environment pressure  $P_0/P_1$ .

The similarities between the factors contributing to the unsteady impulse equation above and the impulse from ideal, steady flow expansion should be noted. Consider a rocket operating at a given environment pressure and assume the combustion products adiabatically expand within the nozzle. Here the energy content of the products is represented by the total enthalpy  $h_t$  which remains constant throughout the nozzle<sup>7,8</sup>. The nozzle area ratio along with the continuity equation and  $\gamma$  of the products determine the degree of product expansion, represented by the ratio of pressure at the nozzle exhaust to the total pressure  $P_t$  in the combustion chamber. If the nozzle expansion ratio is optimized such that the exhaust pressure and the environment pressure are equal then the nozzle area ratio does not need to be known explicitly. Thus, the specific impulse of a steady-flow rocket engine (Eq. 7) depends, as in the case of a detonation tube, on the mixture properties (specific heat ratio  $\gamma$  and energy content  $h_t$ ), and the environment pressure  $P_0/P_t$ .

$$I_{SP} = \frac{1}{g} \sqrt{h_t \left[ 1 - (P_0/P_t)^{(\gamma-1)/\gamma} \right]} \quad (7)$$

While directly comparing the unsteady impulse from a detonation tube to the steady impulse from a rocket is not strictly valid, the fact that both depend on the product specific heat ratio, the energy content in the products and the environment pressure ratio implies that comparisons can be made, if done so carefully. The value of  $\gamma$  remains the same in both the steady and unsteady flow cases. In particular, the initial pressure  $P_1$  of the detonation tube is representative of the combustion pressure as is the total pressure  $P_t$  in the steady flow case. A steady-flow equivalent pressure ratio for the case of the detonation tube is needed to facilitate a meaningful comparison. This is discussed further in a later section.

### III. Experimental Facility

The detonation tube had an inner diameter of 76.2 mm and a length of 1.014 m. One end of the tube was closed, forming the thrust surface, while the other end was open. Mylar diaphragms with thicknesses of 25, 51, and 105  $\mu\text{m}$  initially sealed the open end separating the combustible ethylene-oxygen mixture from the environment air. Three pressure transducers and ten ionization gauges measured wave arrival times and pressure histories at specific axial locations. Mixture ignition occurred at the thrust surface by a standard aircraft spark plug with a discharge energy of 30 mJ. Due to the low spark energy, detonations were obtained by transition from an initial deflagration.

The detonation tube was hung in a ballistic pendulum arrangement within a large tank (the tank was actually the test section and dump tank of the T5 hypersonic wind tunnel facility at Caltech) as illustrated in Fig. 4. The “environment” refers to the volume internal

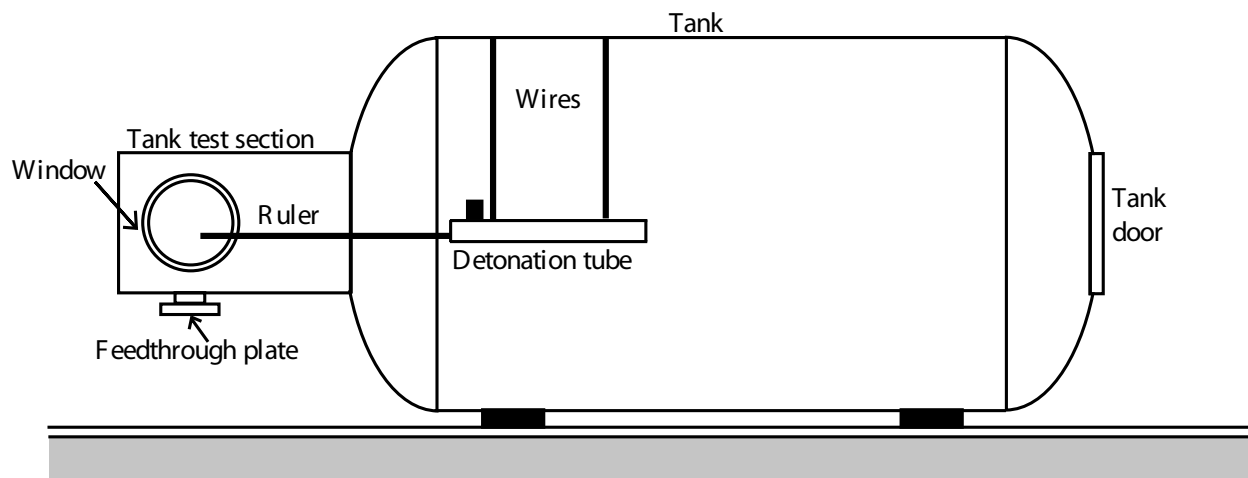


Figure 4. Schematic of Facility II.

to the tank but external to the detonation tube and consisted of room-air at pressure  $P_0$  between 100 and 1.4 kPa. The initial pressure  $P_1$  of the combustible mixture inside the detonation tube varied between 100 and 30 kPa.

The cylindrical tank had an inner diameter of 2 m, a length of 4 m, and an internal volume of approximately 12,500 L. The attached test section (labeled in Fig. 4) is a cylinder approximately 0.7 m in diameter and 1.3 m in length. It incorporated two windows through which the tube motion was observed by means of a ruler extending from the thrust surface. Movement of the ruler was filmed by a digital camera situated outside the tank. The maximum deflection of the tube was converted into impulse (Eq. 8) by applying the classical

analysis of an impulsively-created motion and the conservation of energy.

$$I_{SP} = \frac{M_p}{g\rho_1 V} \sqrt{2gL_p \left( 1 - \sqrt{1 - \left( \frac{\Delta x}{L_p} \right)^2} \right)} \quad (8)$$

This expression is exact and there are no limits on the values of  $\Delta x$ . Actual values of  $\Delta x$  observed in our experiments were between 39 and 292 mm. The experimental uncertainty in the specific impulse was estimated to be  $\pm 3.8\%$ .

A feedthrough plate located on the bottom of the tank test section (Fig. 4) passed the gas lines and electrical connections through the tank wall to the detonation tube. The initial ethylene-oxygen mixture was created by the method of partial pressures in an external mixing vessel. Prior to each test, the tank door was opened and a new diaphragm was installed. The tank door was then sealed and the desired environment pressure was established with a dedicated vacuum pump. The detonation tube was evacuated with a second vacuum pump to at least 133 Pa and then filled from the mixing vessel to the desired initial pressure.

It should be noted that the exhaust of a practical PDE will not be sealed with a diaphragm. However, this experimental setup requires the use of a diaphragm to obtain repeatable single-cycle impulse data. The presence of the diaphragm has a non-negligible effect on the measured impulse as shown in the next section. The qualitative relationship between single-cycle impulse and environment pressure sought in this work is not affected by the diaphragm.

## IV. Experimental data

### A. Measured $U_{CJ}$ and $P_3$ values

The Chapman-Jouguet (CJ) detonation wave velocities of the ethylene-oxygen mixtures were measured from the ionization gauge data and the plateau pressures  $P_3$  were measured from the recorded pressure histories at each initial mixture pressure. The predicted values of the CJ velocity and the plateau pressure, the average measured value, the difference between the maximum and the minimum measured values, and the standard deviation from the mean appear in Tables 1 and 2 respectively.

The relative differences between the measured and predicted detonation velocities are less than 0.05% for the mixtures with an initial pressure 60 kPa and greater. Larger differences are observed for the mixtures with lower initial pressures, but this is expected due to the longer times required for transition to detonation. The relative difference between the measured and predicted plateau pressures is less than 4% for the mixtures with an initial

$P_1$ (kPa)	$U_{CJ}$ from Stanjan <sup>9</sup> (m/s)	Average $U_{CJ}$ Exps. (m/s)	Max - Min $U_{CJ}$ Exps. (m/s)	Std. Dev. of $U_{CJ}$ Exps. (m/s)
100	2376	2375	63	24
80	2365	2366	63	21
60	2351	2350	90	32
40	2331	2351	12	6
30	2317	2352	221	93

**Table 1.** Measured  $U_{CJ}$  data tabulated for different initial pressures of stoichiometric ethylene-oxygen mixtures.

$P_1$ (kPa)	$P_3$ from Model <sup>3</sup> (MPa)	Average $P_3$ Exps. (MPa)	Max - Min $P_3$ Exps. (MPa)	Std. Dev. of $P_3$ Exps. (MPa)
100	1.222	1.202	0.046	0.016
80	0.970	0.982	0.035	0.012
60	0.720	0.746	0.048	0.015
40	0.472	0.523	0.009	0.004
30	0.351	0.398	0.056	0.024

**Table 2.** Measured  $P_3$  data tabulated for different initial pressures of stoichiometric ethylene-oxygen mixtures.

pressure of 60 kPa and greater. The difference is less than 14% for the mixtures with a lower initial pressure. The average measured values for the detonation velocity and plateau pressure were found to be independent of the environment pressure.

### B. $I_{SP}$ measured with 25 and 51 $\mu\text{m}$ diaphragms

Impulse data obtained with the 25 and 51  $\mu\text{m}$  thick diaphragms are plotted in Fig. 5 as a function of  $P_1$ . The data obtained at an environment pressure of 100 kPa agree with previous experimental data<sup>10</sup> obtained in a 50 m<sup>3</sup> blast-proof room within experimental uncertainty. Additional data at environment pressures of 54.5 kPa and 16.5 kPa are shown. The lines are polynomial curve fits to the data.

At an environment pressure of 100 kPa, the specific impulse decreases as the initial mixture pressure decreases. This was noted previously and can be attributed to the increasing importance of dissociation with decreasing initial pressure<sup>10,3</sup>. Because of the low ignition energy, the recorded pressure histories illustrate the major deflagration-to-detonation (DDT) regimes previously<sup>10</sup> documented. DDT was observed in these experiments for mixtures with initial pressures between 30 and 100 kPa. Since the purpose of this study was not to investigate DDT phenomena and the experimental repeatability was poor at conditions of low  $P_0$  and thin diaphragms, the remaining tests were carried out with values of  $P_1 \geq 60$  kPa where

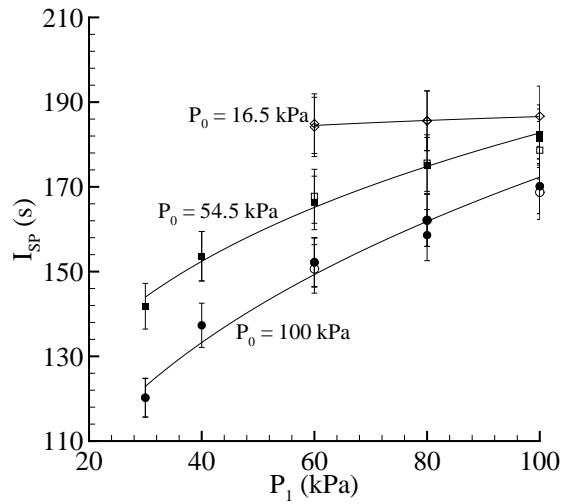


Figure 5. Specific impulse data in tubes with a 25 (solid symbols) or 51  $\mu\text{m}$  (open symbols) thick diaphragm. The initial mixture pressure varied between 100 and 30 kPa and the environment pressure was 100 kPa, 54.5 kPa, or 16.5 kPa.

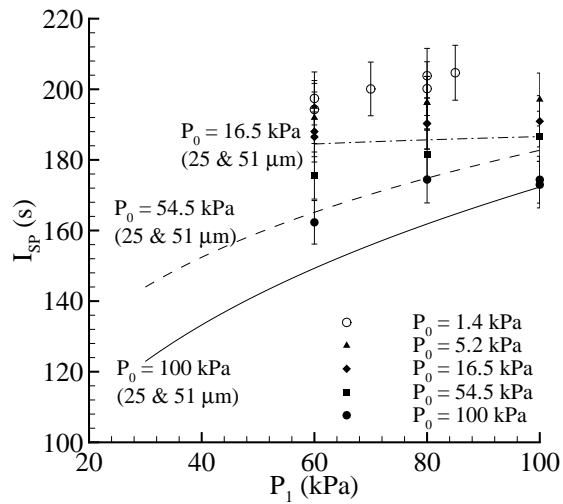
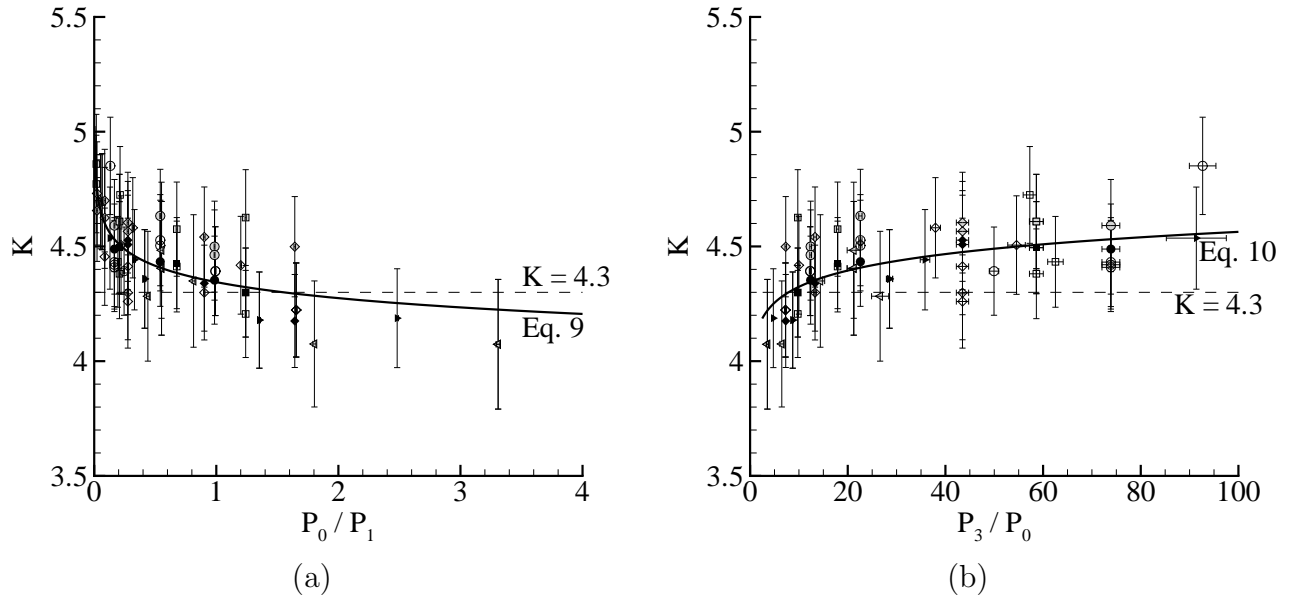


Figure 6. Specific impulse data in tubes with a 105  $\mu\text{m}$  diaphragm as a function of the initial mixture pressure. Data are plotted for environment pressures between 100 kPa and 1.4 kPa.

transition to a detonation occurred within 4 cm of the thrust surface. At lower values of  $P_1$ , DDT occurs later in the tube after a period of flame acceleration and the leading compression waves cause the diaphragm to rupture, spilling some of the unburned mixture outside of the tube. This effect has been previously observed<sup>10</sup> for initial pressures below 30 kPa, but here we observed this effect for initial pressures below 60 kPa when the environment pressure was low. In an effort to prevent early diaphragm rupture at the low environment pressures, a thicker diaphragm of 105  $\mu\text{m}$  was used.

### C. $I_{SP}$ measured with 105 $\mu\text{m}$ diaphragms

Impulse data obtained in tubes sealed with a 105  $\mu\text{m}$  thick diaphragm as a function of the initial mixture pressure appear in Fig. 6. The data at  $P_1 = 100$  kPa with a 105  $\mu\text{m}$  thick diaphragm do not follow the same trend as shown in Fig. 5. This is due to the thicker diaphragm which does not break quickly when the environment pressure is near 100 kPa. The additional time required by the combustion wave to rupture the diaphragm results in energy loss due to heat transfer to the tube walls affecting the experimental repeatability. Evidence of diaphragm melting was observed after the experiments at  $P_0 = 100$  kPa by examining the remaining diaphragm material that was not destroyed by the detonation wave. At the lower environment pressures, evidence of diaphragm melting was not observed and repeat shots generated impulse values within the range of experimental uncertainty.



**Figure 7.** Determination of  $K$  as a function of (a)  $P_0/P_1$  and (b)  $P_3/P_0$  with error bars. Solid lines are the curve fit equations. Open symbols correspond to 25  $\mu\text{m}$  diaphragm, solid black symbols correspond to 51  $\mu\text{m}$  diaphragm, and solid grey symbols correspond to 105  $\mu\text{m}$  diaphragm.

## V. Analysis

### A. Determination of $\beta$

The measured impulse values from Figs. 5 and 6 were used with Eq. 5, and the predicted values of  $U_{CJ}$  and  $P_3$  from Tables 1 and 2 to determine  $K$  as a function of  $P_0$ . The results are plotted in Fig. 7 along with  $K = 4.3$  used in the original impulse model<sup>3</sup>. The scatter

in the data can be attributed to the different diaphragm thicknesses.

A curve fit through the data of Fig. 7(a) yields a relationship (Eq. 9) between  $K$  and the pressure ratio  $P_0/P_1$  which is plotted by the solid line. Alternatively, a relationship (Eq. 10) between  $K$  and the pressure ratio  $P_3/P_0$  is shown by the solid line in Fig. 7(b).

$$K = 4.345 (P_0/P_1)^{-0.023} \quad (9)$$

$$K = 4.345 [(P_0/P_3) \times (P_3/P_1)]^{0.023} \quad (10)$$

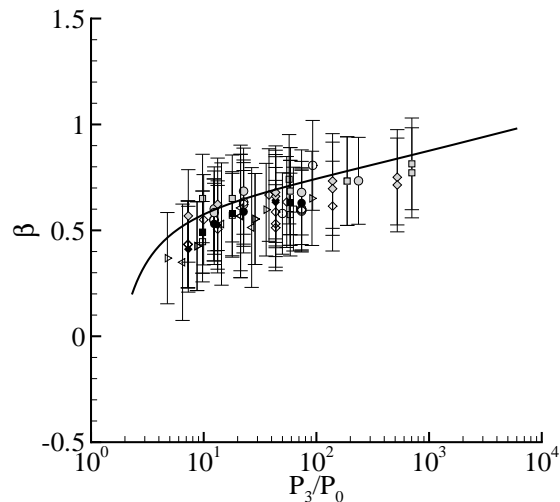


**Figure 8.**  $\beta$  as a function of  $P_3/P_0$ . Open symbols correspond to 25  $\mu\text{m}$  diaphragm, solid black symbols correspond to 51  $\mu\text{m}$  diaphragm, and solid grey symbols correspond to 105  $\mu\text{m}$  diaphragm.

The experimental values of  $\beta$  are calculated with Eq. 6 using a constant value<sup>3</sup> of  $\alpha$  equal to 1.1 and the experimental values of  $K$  (Fig. 7a). Similarly, an empirical relationship for  $\beta$  as a function of  $P_0/P_1$  is determined by using the relationship for  $K$  in Eq. 9 with Eq. 6. Both the individual values of  $\beta$  and the continuous, empirical relationship for  $\beta$  appear in Fig. 8 as a function of  $P_0/P_1$ .

## B. Specific impulse versus $P_0$

The impulse data at initial pressures of 100, 80, and 60 kPa (Figs. 5 and 6) are plotted in Figs. 9-11 as a function of the environment pressure. For each initial pressure, the impulse increases as the environment pressure decreases. Also plotted are the predictions of Eq. 5 with  $\beta = 0.53$  from Wintenberger et al.<sup>3</sup>. A constant value of  $\beta$  results in a linear increase in  $I_{SP}$  with decreasing  $P_0$  for fixed values of  $P_3$  and  $P_1$ . The experimental data best match

the predictions of Eq. 5 with the constant value of  $\beta$  when  $P_0 = P_1$  and the diaphragm is thin. This is expected since these are the conditions under which the parameters  $K$  and  $\beta$  of the original impulse model<sup>3</sup> were derived. The experimental data clearly show an increase in the specific impulse greater than what is predicted if the blow down time  $t_3$  or equivalent  $\beta$  remains constant. The experimental data are predicted if the value of  $\beta$  is defined to be a function of the environment pressure.

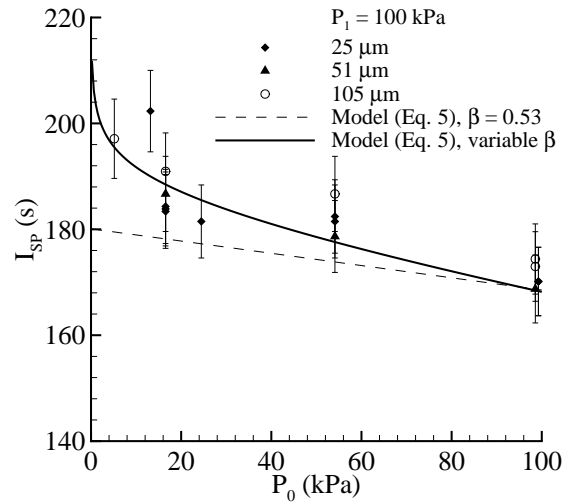


Figure 9. Specific impulse data as a function of  $P_0$  for an initial mixture pressure of 100 kPa.

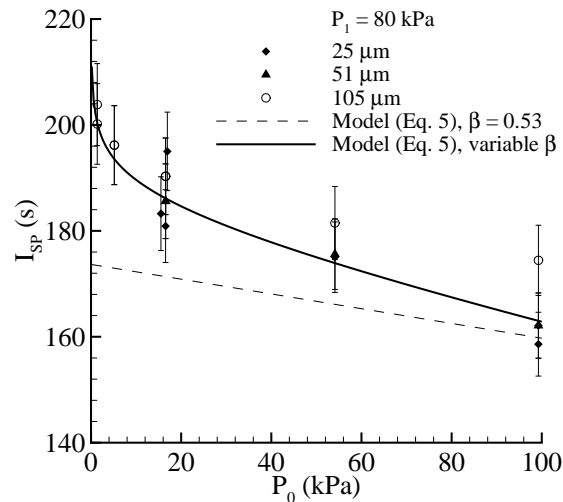


Figure 10. Specific impulse data as a function of  $P_0$  for an initial mixture pressure of 80 kPa.

The data at an initial pressure of 80 kPa are investigated further to determine the relative change in the parameters contributing to the measured impulse. Decreasing the environment pressure from 100 kPa to 1.4 kPa, a 99% decrease, results in the measured impulse increasing

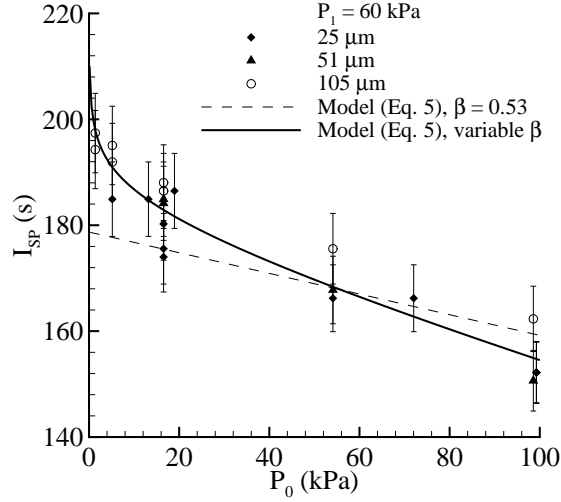


Figure 11. Specific impulse data as a function of  $P_0$  for an initial mixture pressure of 60 kPa.

from 174 s to 202 s, a 16% increase. In the impulse equation (Eq. 5), the only two parameters that change are  $K$  and  $P_0/P_1$ . From Eq. 9,  $K$  increases from 4.323 to 4.769, a 10% increase, due to an increase in the first and third terms of Eq. 6.

### C. Non-dimensionalized impulse data

Non-dimensionalization of the experimental data arises from a key relationship within the impulse model (Eq. 5).

$$\frac{I_{SP}\rho_1gU_{CJ}}{P_1} = K \left( \frac{P_3}{P_1} - \frac{P_0}{P_1} \right) \quad (11)$$

The non-dimensional group  $I_{SP}\rho_1gU_{CJ}/P_1$  appears. The ratio  $P_3/P_1$  is known<sup>3</sup> to depend on  $\gamma$  of the products and the energy content  $q/RT_1$ . Thus, the scaling of Eq. 11 results in Fig. 12 which is plotted as a function of the pressure ratio  $P_0/P_1$ . All data of Figs. 5 and 6 are shown in Fig. 12 and the scatter in the data is due to the different diaphragm thicknesses. The three lines in each series correspond to initial pressures of 100, 80, or 60 kPa.

Alternatively, the impulse can be written as

$$\frac{I_{SP}\rho_1gU_{CJ}}{P_1} = K \left( \frac{P_0}{P_1} \right) \left( \frac{P_3}{P_0} - 1 \right) \quad (12)$$

where the non-dimensional group  $I_{SP}\rho_1gU_{CJ}/P_1$  again appears along with an important pressure ratio  $P_3/P_0$ . Figure 13 replots the data as a function of  $P_3/P_0$  which better illustrates the effect of environment pressure since it is difficult to distinguish the individual data points at pressure ratios  $P_0/P_1 < 0.5$  in Fig. 12.

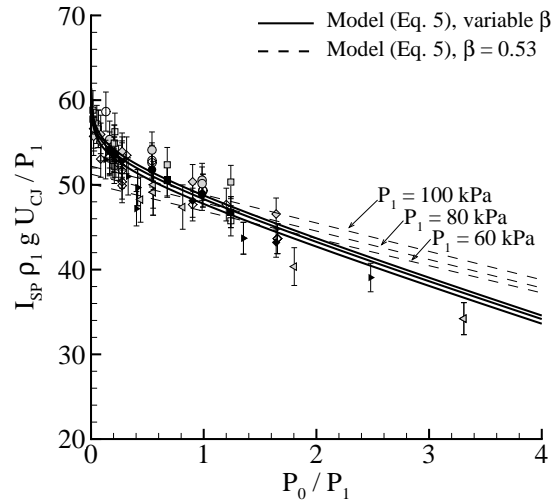


Figure 12. Non-dimensionalized impulse data plotted as a function of  $P_0/P_1$ . Data correspond to initial mixture pressures between 100 and 30 kPa, environment pressures between 100 kPa and 1.4 kPa, and diaphragm thickness of 25 (open symbols), 51 (solid black symbols), and 105  $\mu\text{m}$  (solid grey symbols).

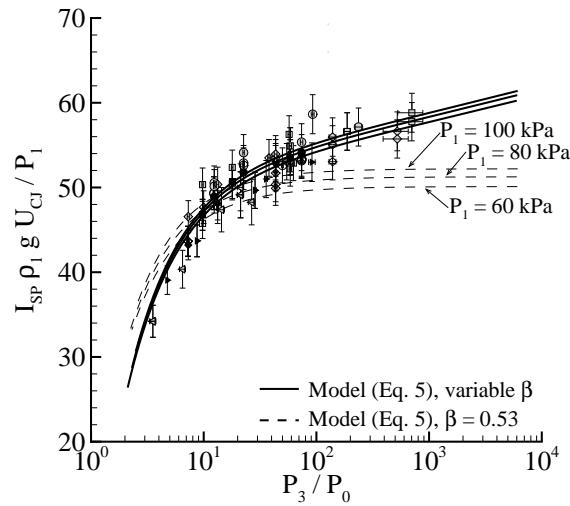


Figure 13. Non-dimensionalized impulse data plotted as a function of  $P_3/P_0$ . Data correspond to initial mixture pressures between 100 and 30 kPa, environment pressures between 100 kPa and 1.4 kPa, and diaphragm thickness of 25 (open symbols), 51 (solid black symbols), and 105  $\mu\text{m}$  (solid grey symbols).

The steady flow predictions for two values of  $h_t$  are plotted with the experimental data in Fig. 14 as a function of  $P_3/P_0$ . While a direct comparison between the steady flow predictions and the detonation tube impulse is not strictly valid, as was discussed previously, the comparison can be used to evaluate the effect of exhaust gas under-expansion and the magnitude of which a perfectly designed nozzle may increase the impulse over the baseline

case of a straight detonation tube. In evaluating the impulse of the steady flow case, a choice for the total enthalpy  $h_t$  must be made that best represents the specific energy content  $q/RT_1$  of the detonation tube. This choice is not straight-forward due to the time-dependency of the flow exiting the detonation tube.

The first obvious choice for  $h_t$  is the condition at state 3, the stagnant flow region behind the Taylor wave. State 3 is present at the thrust surface during a significant fraction of the cycle time  $(t_1 + t_2)/(t_1 + t_2 + t_3)$ . A value of  $h_t = 1264$  kJ/kg is equivalent to state 3 in the detonation tube with an initial mixture of ethylene-oxygen at  $P_1 = 80$  kPa. In this case, the steady flow predictions overestimate the measured impulse data from the detonation tube even at low pressure ratios. This indicates that the chosen value of  $h_t$  does not adequately represent the unsteady case.

A better choice for  $h_t$  would be the average state in the detonation tube during a complete cycle (i.e.  $T = (T_3 + T_0)/2, P = (P_3 + P_0)/2$ ). This is because the average condition inside the detonation tube is at a pressure lower than state 3 since the products are exhausting from the tube during most of the cycle time. For  $P_1 = 80$  kPa, using the average pressure inside the detonation tube results in  $h_t = 690$  kJ/kg. This is plotted in Fig. 14 and better represents the experimental data.

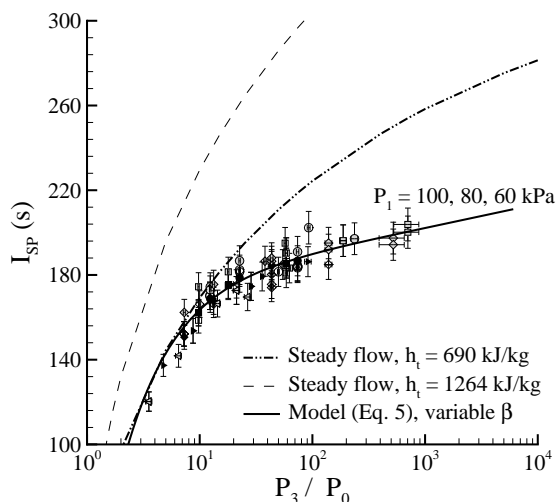


**Figure 14.** Specific impulse data plotted as a function of  $P_3/P_0$ . Data correspond to initial mixture pressures between 100 and 30 kPa, environment pressures between 100 kPa and 1.4 kPa, and diaphragm thickness of 25 (open symbols), 51 (solid black symbols), and 105  $\mu\text{m}$  (solid grey symbols). Thin solid curves corresponds to ideal impulse from a steady flow nozzle for values of  $h_t = 1264$  and 690 kJ/kg. Thick solid curve corresponds to the model predictions with variable  $\beta_{LP}$ .

As the pressure ratio across the nozzle increases, the difference between the experimental data and the theoretical, steady flow impulse increase indicating the lack of complete product gas expansion to the lower environment pressures. This experimental data of a detonation

tube at different environment pressures serves as a baseline from which the effect of adding a nozzle can be quantified.

## VI. Summary

This study obtained the first experimental data quantifying the effect of environment pressure on the single-cycle impulse of a fully filled detonation tube. Data were obtained for stoichiometric mixtures of ethylene-oxygen at initial pressures between 100 and 30 kPa and environment pressures between 100 kPa and 1.4 kPa. The specific impulse increased as the environment pressure decreased and the initial mixture pressure remained constant. This increase in impulse was not predicted by the original impulse model<sup>3</sup> which used a constant value of  $K$  and  $\beta$ . At the lowest environment pressures, the increased blow down time caused the impulse to increase approximately 11% greater than the original impulse predictions. New model parameters  $K = K(\gamma, q/RT_1, P_0/P_1)$  and  $\beta = \beta(\gamma, q/RT_1, P_0/P_1)$  were determined from the experimental data and defined to be functions of the environment pressure. Impulse predictions assuming full expansion from an average condition inside the detonation tube were compared to the impulse of a detonation tube indicating that the detonation tube exhaust products are under expanded.

## VII. Acknowledgment

This work was supported by the Office of Naval Research Multidisciplinary University Research Initiative *Multidisciplinary Study of Pulse Detonation Engine* (N00014-02-1-0589), and General Electric contract GE-PO A02 81655 under DABT-63-0-0001.

## References

- <sup>1</sup> Wintenberger, E., *Application of Steady and Unsteady Detonation Waves to Propulsion*, Ph.D. thesis, California Institute of Technology, 2004.
- <sup>2</sup> Wu, Y., Ma, F., and Yang, V., “System Performance and Thermodynamic Cycle Analysis of Air-Breathing Pulse Detonation Engines,” *Journal of Propulsion and Power*, Vol. 19, No. 4, 2003, pp. 556–567.
- <sup>3</sup> Wintenberger, E., Austin, J. M., Cooper, M., Jackson, S., and Shepherd, J. E., “Analytical Model for the Impulse of a Single-Cycle Pulse Detonation Tube,” *Journal of Propulsion and Power*, Vol. 19, No. 1, 2003, pp. 22–38.
- <sup>4</sup> Falempin, F., Bouchaud, D., Forrat, B., Desbordes, D., and Daniau, E., “Pulsed Detona-

- tion Engine Possible Application to Low Cost Tactical Missile and to Space Launcher,” 37th AIAA/ASME/SAE/ASEE Joint Propulsion Conference and Exhibit, July 8–11, 2001, Salt Lake City, UT, AIAA 2001–3815.
- <sup>5</sup> Wintenberger, E., Austin, J. M., Cooper, M., Jackson, S., and Shepherd, J. E., “Reply to Comment on “Analytical Model for the Impulse of Single-Cycle Pulse Detonation Tube (Wintenberger et al., *Journal of Propulsion and Power*, Vol. 19, No. 1, pp. 22–38, 2003), by W. H. Heiser and D. T. Pratt,” *Journal of Propulsion and Power*, Vol. 20, No. 1, 2004, pp. 189–191.
  - <sup>6</sup> Wintenberger, E., Cooper, M., Pintgen, F., and Shepherd, J. E., “Reply to Comment on “Analytical Model for the Impulse of Single-Cycle Pulse Detonation Tube (Wintenberger et al., *Journal of Propulsion and Power*, Vol. 19, No. 1, pp. 22–38, 2003), by M. I. Radulescu and R. K. Hanson,” *Journal of Propulsion and Power*, Vol. 20, No. 5, 2004, pp. 957–959.
  - <sup>7</sup> Sutton, G. P., *Rocket Propulsion Elements*, John Wiley and Sons, Inc., New York, NY, sixth ed., 1992, pp. 41–68.
  - <sup>8</sup> Hill, P. G. and Peterson, C. R., *Mechanics and Thermodynamics of Propulsion*, Addison-Wesley, 2nd ed., 1992, pp. 513–540.
  - <sup>9</sup> Reynolds, W., “The element potential method for chemical equilibrium analysis: implementation in the interactive program STANJAN,” Tech. rep., Mechanical Engineering Department, Stanford University, 1986.
  - <sup>10</sup> Cooper, M., Jackson, S., Austin, J. M., Wintenberger, E., and Shepherd, J. E., “Direct Experimental Impulse Measurements for Detonations and Deflagrations,” *Journal of Propulsion and Power*, Vol. 18, No. 5, 2002, pp. 1033–1041.